EXPERIMENTAL CELL RESEARCH 312 (2006) 1514–1525

available at www.sciencedirect.com

SCIENCE DIRECT®

www.elsevier.com/locate/yexcr

Research Article

Glycogen synthase kinase-3 acts upstream of ADP-ribosylation factor 6 and Rac1 to regulate epithelial cell migration

*Rizwan Farooqui, Shoutian Zhu, Gabriel Fenteany**

Department of Chemistry, University of Illinois, Chicago, IL 60607, USA

ARTICLE INFORMATION

Article Chronology:
Received 26 November 2005
Revised version received
16 January 2006
Accepted 17 January 2006
Available online 9 March 2006

Keywords:
Epithelial wound closure
Cell sheet migration
Cell scatter
GSK-3
Rac1
ARF6
HGF/SF

Abbreviations:
ARF6, ADP-ribosylation factor 6
GSK-3, glycogen synthase kinase-3
HGF/SF, hepatocyte growth factor/scatter factor
MDCK, Madin–Darby canine kidney
P13K, phosphatidylinositol 3-kinase

ABSTRACT

Cell sheet movement during epithelial wound closure is a complex process involving collective cell migration. We have found that glycogen synthase kinase-3 (GSK-3) activity is required for membrane protrusion and crawling of cells at the wound edge and those behind it in wounded Madin–Darby canine kidney (MDCK) epithelial cell monolayers. RNA interference-based silencing of GSK-3α and GSK-3β expression also results in slowed cell sheet migration, with the effect being more pronounced with knockdown of GSK-3β. Both GSK-3α and GSK-3β are in activated states during the most active phase of cell migration. In addition to having a positive control or permissive, rather than negative, function in MDCK cell migration, GSK-3 appears to act upstream of the small GTPases ADP-ribosylation factor 6 (ARF6) and Rac1. Expression of constitutively active ARF6 restores a protrusive, migratory phenotype in cells treated with GSK-3 inhibitors. It does not, however, restore to normal levels the directional polarization of cells behind the wound edge toward the wound area, implying the existence of a separate ARF6-independent branch of the GSK-3 pathway that regulates proper wound-directed polarization of these cells. Finally, inhibition of GSK-3 also strongly reduces activation of Rac1 and cell scatter in response to hepatocyte growth factor/scatter factor, which triggers dispersal and migration of cells in monolayer culture as fibroblast-like individual cells, a mode of epithelial cell motility distinct from the collective migration of wound closure.

Introduction

Glycogen synthase kinase-3 (GSK-3) is an important regulator of various signal transduction pathways, regulating processes such as insulin-dependant glycogen synthesis, microtubule function, cell polarity, cell adhesion, cell survival, protein synthesis and the function of certain transcription factors (for reviews, see Refs. [1–3]). Improper GSK-3 signaling has been associated with diseases like Alzheimer's, bipolar disorder and type II diabetes, making it an attractive target

* *Corresponding author.*
E-mail address: fenteany@uic.edu (G. Fenteany).

0014-4827/$ – see front matter © 2006 Elsevier Inc. All rights reserved.
doi:10.1016/j.yexcr.2006.01.018

for therapeutic intervention (for reviews, see Refs. [4–8]). GSK-3 is generally active in resting-state cells; upon cell stimulation, GSK-3 is inactivated, thus releasing the signaling pathways it otherwise negatively regulates. Inactivation of GSK-3 occurs through phosphorylation of an N-terminal serine: specifically, Ser 21 of the α isoform and Ser 9 of the β isoform of GSK-3.

GSK-3 is a downstream effector in the Cdc42-dependent regulation of microtubule function and cell polarity (for a review, see Ref. [9]). Cdc42, along with the related Rac and Rho proteins, is a small GTPase that controls cytoskeletal dynamics (for reviews, see Refs. [10–14]). During migration of primary rat astrocytes, signaling through Cdc42 at the cells' leading edge results in inactivating phosphorylation of GSK-3β, which promotes the microtubule-stabilizing interaction of the adenomatous polyposis coli protein with the growing ends of microtubules in the direction of cell protrusion and migration [15]. In addition to the link between Cdc42 and GSK-3, there may be a different kind of inter-relationship between Rac and GSK-3. In cultured human keratinocytes, epidermal growth factor- and staurosporine-induced cell migration after scratch wounding, translocation of Rac1 and formation of extended lamellipodia are prevented by chemical inhibition of GSK-3, implying that GSK-3 functions as a positive regulator upstream of Rac1 in this pathway to epithelial cell motility [16,17].

Following wounding of Madin–Darby canine kidney (MDCK) epithelial cell monolayers, cells move in to close the gap as a continuous sheet, strictly maintaining cell–cell contacts. Wound closure in MDCK cell monolayers is driven exclusively by cell migration, with active protrusive crawling in multiple rows of cells from the wound edge, and not by purse-string contraction or cell proliferation [18,19]. MDCK cell sheet migration depends on Rac and phosphoinositides [18], c-Jun-N-terminal kinase [20] and Raf kinase inhibitor protein [21,22]. Furthermore, Santy and Casanova have shown that another small GTPase, ADP-ribosylation factor 6 (ARF6), is required for MDCK cell sheet migration and that it acts upstream of Rac1 in this process [23].

Here we present evidence showing that GSK-3 is involved in MDCK cell sheet migration. Treatment with inhibitors of GSK-3 inhibits cell sheet migration during wound closure. Membrane protrusion, both the lamellipodial extension at the wound edge and the cryptic protrusion of cells behind the edge, is reduced with inhibition of GSK-3. siRNA-mediated silencing of the expression of GSK-3α or GSK-3β, particularly the latter, also reduces the rate of cell sheet migration. The phosphorylation states of GSK-3α and GSK-3β change over the course of wound closure, with a pattern that indicates that they are both activated during the most active phase of cell migration. Expression of a constitutively active mutant of ARF6 (ARF6-CA) restores a migratory phenotype in cells treated with GSK-3 inhibitors, although it does not restore normal levels of directional polarization of cells behind the wound margin toward the wound area. As with the results of Koivisto et al. in keratinocytes [16,17], our data are consistent with a positive control or permissive, rather than negative, function for GSK-3 in epithelial cell migration. Furthermore, treatment of epithelial cells with hepatocyte growth factor/scatter factor (HGF/SF) is known to trigger an epithelial–mesenchymal-like transition in MDCK in two-dimensional cultures, with loss of cell–cell adhesions and cell scatter [24–27]. The HGF/SF-stimulated epithelial cells move as single individuals rather than collectively as in wound closure. We found that in subconfluent MDCK cell cultures, GSK-3 inhibitors markedly reduced levels of activated Rac1, both the low basal amount and the elevated level following treatment with HGF/SF. These results suggest that GSK-3 acts upstream of ARF6 and Rac1 in the regulation of MDCK cell migration and that a separate ARF6-independent branch of the GSK-3 pathway is important for wound-directed polarization of cells behind the wound edge.

Materials and methods

Reagents

Minimum essential medium (MEM, with Earle's balanced salts, nonessential amino acids, L-glutamine, sodium pyruvate and 2.1 g/l sodium bicarbonate) and lipofectamine were purchased from Invitrogen/Gibco. Newborn calf serum (NCS) was from Biowhittaker. GSK-3 inhibitor IX, SB415286 and wortmannin were obtained from EMD Biosciences/Calbiochem. Anti-GSK-3α/β antibody and anti-hemagglutinin (HA), horseradish peroxidase (HRP)-conjugated donkey anti-rabbit IgG and HRP-conjugated goat anti-mouse IgG secondary antibodies were purchased from Santa Cruz Biotechnology. Anti-phospho-GSK-3α (Ser 21) and anti-phospho-GSK-3β (Ser 9) anti-phospho-GSK-3α/β (Ser21/9) antibodies were from Cell Signaling Technology, and anti-Rac1 antibody was from BD Biosciences. Anti-actin antibody was from Sigma-Aldrich. Alexa Fluor 350-conjugated anti-IgG secondary antibody was from Invitrogen/Molecular Probes. The plasmid pcDNA3 encoding enhanced green fluorescent protein (GFP)-human β-actin described previously [28] was modified to contain the hygromycin resistance gene derived from pTRE2HYG (Clontech Laboratories).

Cell culture

MDCK (strain II) epithelial cells stably transfected with the tetracycline-controlled transactivator protein (MDCK Tet-Off cells, originally known as MDCK T23 cells) [29] were purchased from Clontech Laboratories. These cells allow for inducible expression of tetracycline-responsive promoter-controlled transgenes, which was critical for the experiments involving adenoviral gene transfer. In the Tet-Off system, transgene expression is only activated in the absence of tetracycline or its analog doxycycline. For consistency, we used MDCK Tet-Off cells throughout this study, even for experiments not involving gene transfer and regulated gene expression. Cells were maintained in growth medium consisting of MEM with 10% NCS and grown at 37°C in a humidified tissue culture incubator with 5% CO2. Cells were not used beyond 12 passages from thaw of frozen stock cultures (stored in liquid N_2).

Wound closure/cell sheet migration assay

MDCK cells were plated in Bioptechs delta T culture dishes in growth medium. At confluence, cells were rinsed and

incubated with serum-free MEM. After 36 h of serum starvation, cells were wounded in the presence or absence of different inhibitors. The wounds (~700-μm width by ~18-mm length) were made by scratching the monolayer with a flame-blunted microinjection needle attached to a Narishige micromanipulator. Culture dishes were maintained at 37°C in a Bioptechs Delta TC3 stage heater, and images were captured over a 12-h period with a Zeiss Axiovert 200 microscope with Uniblitz shutter (Vincent Associates), Zeiss AxioCam HR cooled CCD camera and Openlab software (Improvision). The rate of overall cell sheet migration in the "forward" direction was measured by imposing a grid onto each image using the public domain ImageJ program (developed at the National Institutes of Health and available on the Internet at http://rsb.info.nih.gov/ij/). The rate of uni-directional movement of the wound edge forward along 10 different evenly spaced parallel lines, all perpendicular to the wound edge, was determined for a 12-h period for each experiment. The average rate of cell sheet migration was calculated for the forward progress of all the wound-edge points from at least three separate experiments in each case. The procedures outlined above were followed for all cell sheet migration experiments, including those using adenovirus-infected or siRNA-expressing MDCK cells.

Stable transfection of GFP-actin into MDCK Tet-Off cells

We generated MDCK Tet-Off cells constitutively expressing GFP-actin by lipofectamine-mediated transfection, according to the manufacturer's protocol (Gibco/Invitrogen), to allow for subsequent inducible expression of an ARF6-CA transgene and fluorescence analysis of membrane protrusion, as previously described [19]. Selection and maintenance of stable transfectants were done in growth medium containing 400 μg/ml hygromycin. GFP-actin-positive cells were isolated with a DakoCytomation MoFlo fluorescence-activated cell sorter (FACS).

Adenoviral gene transfer

Adenovirus production and adenoviral gene transfer into MDCK Tet-Off cells were done as previously described [23,30]. Briefly, the cells were plated on glass slides in 12-well plates or directly onto Bioptechs Delta T culture dishes. The cells consisted of a mixture of GFP-actin-expressing and non-GFP-actin-expressing cells in a 1:10 ratio for the experiments described in Fig. 2 and Table 1. After reaching confluence, the cells were serum starved for 36 h, then infected for 2 h with adenovirus encoding HA-tagged ARF6-CA (ARF6Q67L) under the control of a tetracycline-responsive promoter, diluted in Hanks balanced salt solution. A viral titer that resulted in approximately 80–90% infection was used, as determined empirically by staining for HA, using a previously described immunofluorescent staining procedure [31].

Wounding and fluorescence analysis of membrane protrusion

After adenoviral infection, the cells were rinsed, and fresh serum-free medium containing inhibitor or dimethyl sulfoxide (DMSO) was added. To control for any possible effects of adenoviral infection, ARF6-CA expression was prevented in control plates by maintaining cells in 1 μg/ml doxycycline throughout the experiment. Fresh inhibitor and medium were added after 10 h, and the monolayers were wounded with a flame-blunted microinjection needle. The cells were fixed 12 h later with 3.7% formaldehyde (in PBS, as were subsequent solutions), washed, permeabilized with 0.5% Triton X-100 and stained for filamentous actin (F-actin) with tetramethylrhodamine isothiocyanate-labeled phalloidin (TRITC-phalloidin) and for the HA epitope with anti-HA antibody and Alexa Fluor 350-conjugated secondary antibody.

Analysis of membrane protrusion from cells at and behind the wound edge was performed as previously described [19]. The experiments presented here were done under serum-free conditions. We have previously shown that serum deprivation results in increased membrane protrusion at the wound edge but does not affect the rate of MDCK cell sheet migration during wound closure [20].

Reverse transcriptase-polymerase chain reaction (RT-PCR)

GSK-3 isoform-specific RT-PCR was performed with mRNA from MDCK cells purified with the Qiagen RNeasy Mini kit. Moloney murine leukemia virus reverse transcriptase and oligo(dT) or random hexamer primers were used for cDNA synthesis, according to the manufacturer's protocol (Promega). PCR reactions were performed using primers designed to span an intron and allow differentiation between cDNA and any contaminating genomic products. For GSK-3α, the forward primer was 5′-AACCGAGAGCTGCAGATT-3′ and the reverse primer was 5′-AATGGACGAGGTGTAATC-3′. For GSK-3β, the forward primer was 5′-GATTCGTCAGGAACAGGAC-3′ and the reverse primer was 5′-CTTGAGTGGTGAAGTTGAA-3′. PCR products were visualized on agarose gels with ethidium bromide and UV transillumination.

RNA interference (RNAi)-based silencing of GSK-3α and GSK-3β expression

Silencing of GSK-3α and GSK-3β expression was achieved using a small hairpin RNA (shRNA) expression vector modified from that previously described [22]. The tetracycline-responsive element and multiple cloning site were removed with *Sma*I and *Eco*RV and replaced with the U6 promoter and multiple cloning site from Ambion's pSilencer 2.0 U6 (excised with *Pvu*II). A point mutation in the *Hin*dIII restriction site upstream of the hygromycin-resistance gene was introduced to ensure that the only restriction site for *Hin*dIII remained in the multiple cloning site. Potentially effective small interfering RNA (siRNA) target sequences corresponding to different parts of the coding regions of each GSK-3 isoform, and not found elsewhere in the canine genome, were identified with Ambion's siRNA Target Finder algorithm. For each GSK-3 isoform, four different siRNA target sequences were synthesized as shRNAs and ligated into the shRNA expression vector between its *Hin*dIII and *Bam*HI sites; the constructs were then separately transfected into the MDCK cells by lipofectamine-mediated transfection, according to the manufacturer's protocol (Gibco/Invitrogen). Stable transfectants were selected in

growth medium with 400 μg/ml hygromycin. Since the shRNA expression vector contains a GFP expression cassette [22], GFP-positive cells were isolated by FACS. Efficiency of knockdown was evaluated by Western blot analysis. The best knockdown of GSK-3α was achieved with an siRNA corresponding to nucleotides 376–396 GSK-3α transcript variant 1 (Genbank accession XM_541590), a sequence also present in GSK-3α transcript variant 2 (Genbank accession XM_847613). The siRNA yielding the best knockdown of GSK-3β corresponded to nucleotides 155–175 of the coding region of GSK-3β transcript variant 1 (Genbank accession XM_535751). All GSK-3β transcript variants except variant 3, which encodes a smaller 36-kDa protein, possess this sequence. As a control for the subsequent wound closure experiments, we used a cell line expressing an siRNA corresponding to nucleotides 962–982 of GSK-3α transcript variant 2, which we found to cause no change in GSK-3α protein levels (data not shown). Each cell line was maintained in growth medium containing 400 μg/ml hygromycin.

Preparation of wounds for GSK-3 phosphorylation and Rac1 activation assays

10-cm-diameter tissue culture plates were plated with 4×10^6 MDCK cells/plate in growth medium and grown to confluence, followed by 36-h serum starvation. Fresh serum-free medium was then added with or without inhibitor. The monolayers were multiply wounded using a flame-blunted microinjection needle with ~30 wounds/plate across each plate, basically as previously published [20]. This wounding procedure allowed a large number of wounds to be generated without causing the entire monolayer to be damaged or lift off. The wounds extended from one end of the plate to the other and were approximately parallel with ~3 mm between wounds. In addition, the specific width of the wounds could be controlled by preparing microinjection needles with different thicknesses of the flame-blunted tip.

Detection of GSK-3 phosphorylation

At different times after generating ~30 wounds/plate as described above, the cells were rinsed with ice-cold phosphate-buffered saline (PBS) and then lysed with 200 μl/plate of 2× sodium dodecyl sulfate (SDS) sample buffer. The lysates were boiled for 10 min and sonicated for 15 min in a sonicating water bath. They were then centrifuged for 15 min at 16.3 × 1000 × *g* and subjected to SDS-12% polyacrylamide gel electrophoresis. Proteins were then transferred electrophoretically to polyvinylidene fluoride membranes overnight. The blots were blocked with 5% skim milk in Triton X-100-Tris-buffered saline (T-TBS) for 1 h. Anti-phospho-GSK-3α, anti-phospho-GSK-3β, anti-phospho-GSK-3α/β and anti-GSK-3α/β were used to probe separate blots of gels loaded with equivalent amounts of the same lysates. Each antibody was diluted 1:500 in 5% bovine serum albumin in T-TBS, followed by incubation for 24 h at 4°C. HRP-conjugated secondary antibody was diluted 1:1000 in 5% skim milk and incubated on the blots for 2 h at room temperature before enhanced chemiluminescence detection according to the manufacturer's procedure (Amersham/GE Healthcare).

Rac1 activation assay

At different times after preparation of ~30 wounds/plate as described above, cells were rinsed with ice-cold PBS and lysed. In contrast, for experiments involving HGF/SF, cells were seeded at 1×10^6 cells for each 10-cm-diameter tissue culture plate and incubated in growth medium for 24 h to ~40% confluence. 25 ng/ml HGF/SF was then added in the presence or absence of inhibitor. After another 24 h, cells were lysed. In both types of experiments, following cell lysis, activated Rac1 was then isolated by an affinity pull-down assay with an immobilized GST fusion protein containing the p21 (Cdc42/Rac1) binding domain (PBD) of PAK3, as previously described [32], and then detected by Western blot analysis with anti-Rac1 antibody. Corresponding total Rac1 was determined by Western blot analysis of the crude cell lysates with anti-Rac1 antibody.

Results and discussion

Inhibition of GSK-3 signaling inhibits cell sheet migration and wound closure

Treatment of wounded MDCK epithelial cell monolayers with 1 μM GSK-3 inhibitor IX, a potent and selective inhibitor of GSK-3 [33], resulted in inhibition of cell sheet migration during wound closure (measured as overall progress of the sheet in the "forward" direction), with a rate of 0.25 ± 0.01 μm/min for mean ± standard error of the mean (SEM) compared to 0.59 ± 0.02 μm/min for the control (Fig. 1). Treatment with 40 μM SB415286, another GSK-3 inhibitor [34], also resulted in inhibition, with a rate of 0.17 ± 0.01 μm/min (mean ± SEM) (Fig. 1). At the end of each experiment, cell viability was evaluated by observation of cell morphology and the Trypan blue dye exclusion assay, and there was no sign of cytotoxicity with either GSK-3 inhibitor at the concentrations used even after 36-h treatment.

Inhibition of GSK-3 results in reduced marginal and submarginal membrane protrusion

Treatment of MDCK cells with GSK-3 inhibitor IX or SB415286 inhibited lamellipodial extension in cells at the wound edge or margin (marginal cells) and those behind the wound margin (submarginal cells) during cell sheet migration (Fig. 2 and Table 1). Submarginal lamellipodia are cryptic membrane protrusions emanating from multiple rows of cells behind the wound edge, and these protrusions are wedged under cells in front of them [19]. The strongest inhibitory effect of the GSK-3 inhibitors was observed at the wound margin (Table 1). Inhibition of GSK-3 also decreased protrusive activity behind the wound edge (Table 1), down to a "background" level similar to that found in unwounded monolayers [19]. Of those submarginal cells that protrude, there appears a decrease in directional polarization of the cells toward the wound area upon treatment with the GSK-3 inhibitors (Table 1). Time-lapse sequences following wounding of monolayers also revealed a marked decrease in the number of lamellipodia that form at the margin per unit

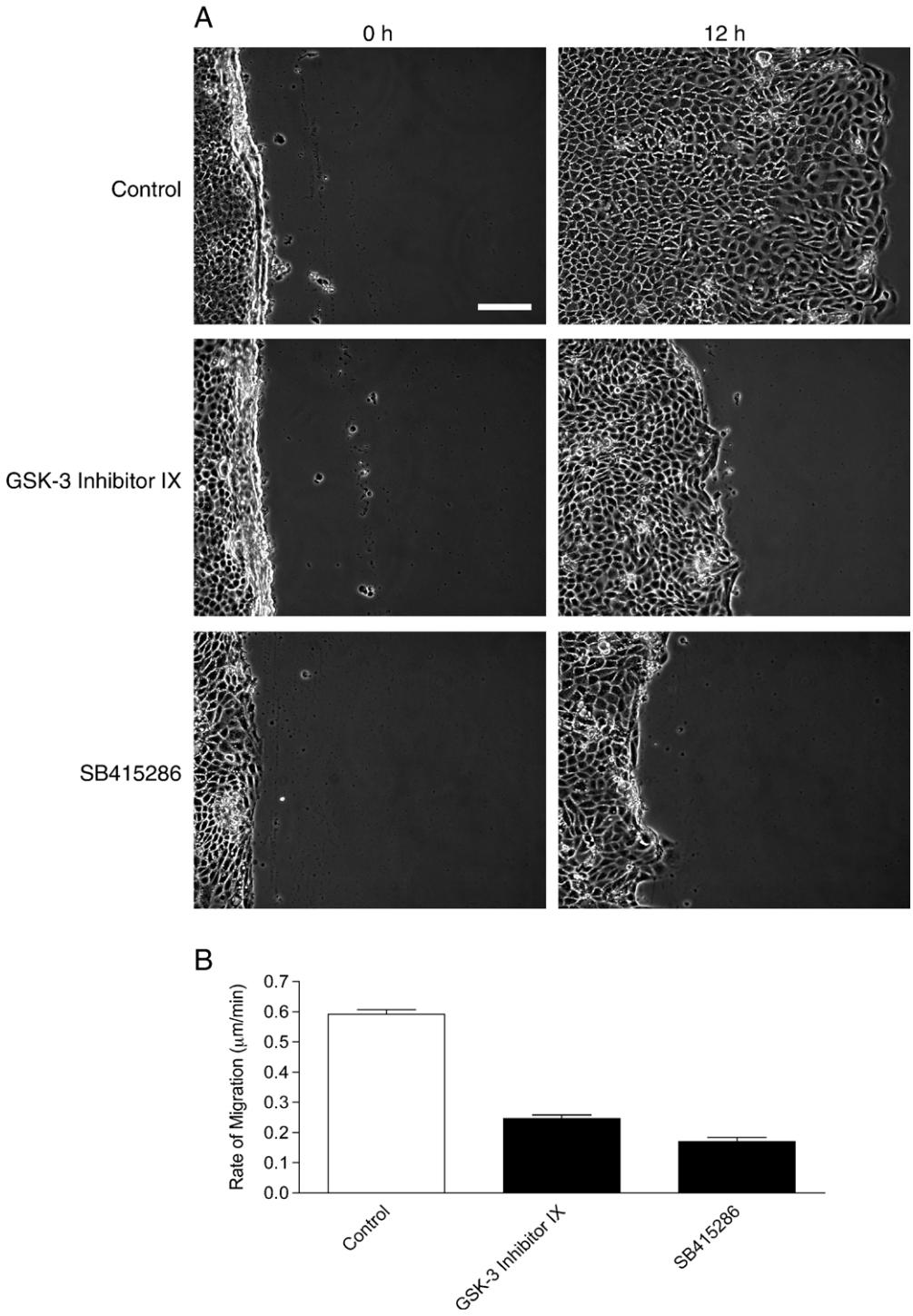

Fig. 1 – Inhibition of GSK-3 inhibits epithelial cell sheet migration. (A) Confluent MDCK cell monolayers were treated with 0.2% DMSO carrier solvent, 1 μM GSK-3 inhibitor IX or 40 μM SB415286 and then scratch wounded. Time-lapse images were acquired over a 12-h period, with representative images shown. Scale bar = 100 μm. (B) The rate of overall cell sheet migration in the "forward" direction during wound closure was calculated from the time-lapse images, as described in Materials and methods, and is represented as mean ± SEM for three separate experiments for each treatment. In addition, we found partial restoration of the normal rate of cell sheet migration with infection of cells with adenovirus containing a constitutively active mutant of ARF6 (ARF6-CA), followed by treatment with 40 μM SB415286: the rate (mean ± SEM) of cell sheet migration increased from 0.17 ± 0.01 μm/min to 0.29 ± 0.02 μm/min μm/min with expression of ARF6-CA in inhibitor-treated cells. (See Fig. 2, Table 1 and the text for details about experiments involving adenoviral infection. Since MDCK Tet-Off cells were important for inducible gene expression in the adenoviral infection experiments, we used MDCK Tet-Off cells for all experiments in this study to maintain consistency.)

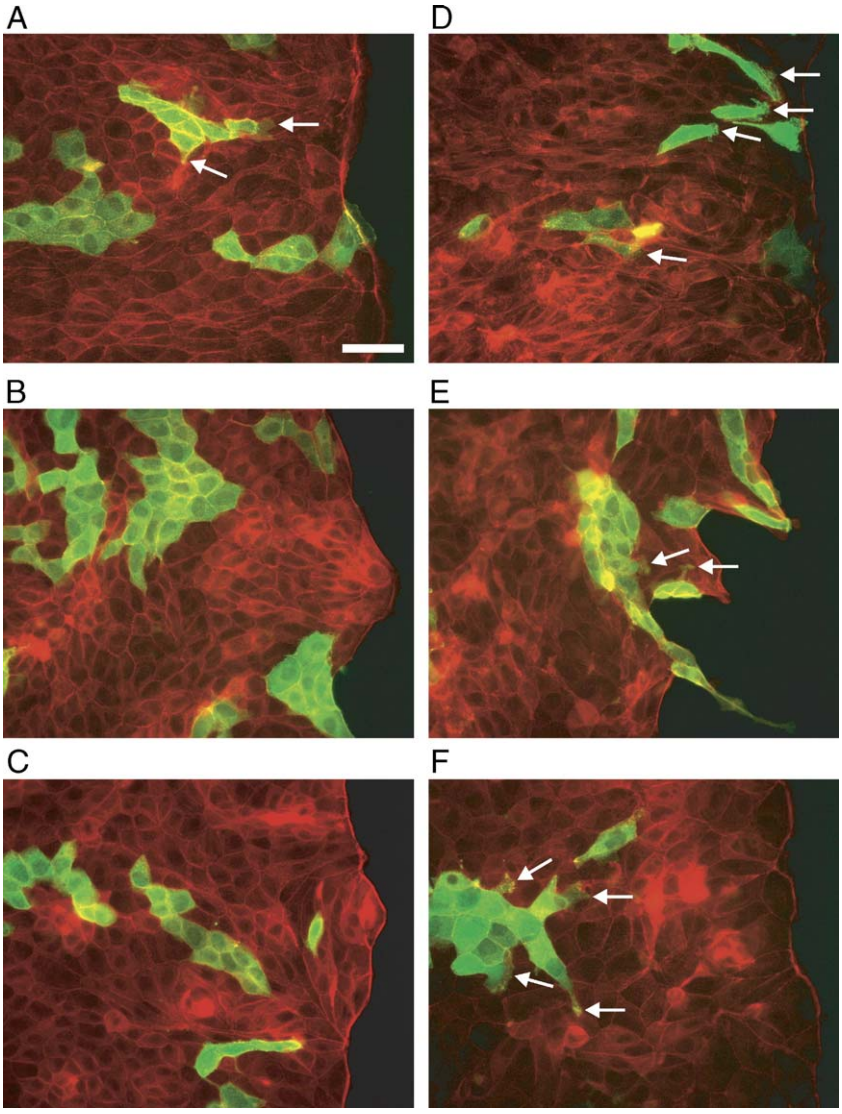

Fig. 2 – Membrane protrusion is reduced in the presence of GSK-3 inhibitors at and behind the wound edge but is restored with simultaneous expression of ARF6-CA. Confluent MDCK cell monolayers consisting of GFP-actin-expressing cells (green) and non-GFP-actin-expressing cells in a 1:10 ratio were infected with adenovirus encoding HA-tagged ARF6-CA under the control of a tetracycline-responsive promoter. Cells were then treated with: (A) 0.2% DMSO with doxycycline (to prevent ARF6-CA expression in controls for panels D–F); (B) 2.5 μM GSK-3 inhibitor IX, doxycycline; (C) 40 μM SB415286, doxycycline; (D) 0.2% DMSO, ARF6-CA; (E) 2.5 μM GSK-3 inhibitor IX, ARF6-CA; (F) 40 μM SB415286, ARF6-CA. Cell monolayers were wounded and fixed 12 h later, then permeabilized and stained for F-actin (red) and the HA epitope (data not shown). Infection efficiency was typically 80–90%. Submarginal protrusions are indicated with arrows. Scale bar = 50 μm.

length of margin (lamellipodial density) after treatment with the GSK-3 inhibitors (data not shown).

Expression of ARF6-CA restores a migratory phenotype in cells treated with GSK-3 inhibitors

The small GTPase ARF6 has been shown to regulate MDCK cell sheet migration during wound closure [23] and is also involved in HGF/SF-stimulated MDCK cell scattering [35]. ARF6 is activated by the ARF-specific guanine nucleotide exchange factor ARNO, leading to activation of Rac1 during MDCK cell sheet migration [23] through a bipartite Rac guanine nucleotide exchange factor, the Dock180/Elmo complex [36].

As a first step toward establishing how GSK-3 signaling is integrated with the ARF6 pathway, we used adenovirus-mediated gene transfer to deliver ARF6-CA into MDCK Tet-Off cells that were treated with DMSO carrier solvent alone, GSK-3 inhibitor IX or SB415286. Expression of ARF6-CA by itself results in increased proportion of protruding cells compared to the controls (ARF6-CA/DMSO compared to doxycycline/DMSO in Table 1). Moreover, we found that ARF6-CA expression restored the protrusive phenotype of cells treated with GSK-3 inhibitors by multiple measures of protrusion, including frequency of membrane protrusion and the length and area of the protrusions (Table 1). In addition, we found partial restoration of the normal rate of overall cell

Table 1 – Parameters of membrane protrusion in cells at and behind the wound edge during wound closure

Distance from the wound margin [a]	% cells protruding [b]	% Protrusions oriented toward the wound [c]	Average length (μm) [d]	Average area (μm^2) [e]
Doxycycline/DMSO				
Marginal	62.3 ± 2.1 (*n* = 31 slides)	100	11.3 ± 0.5 (*n* = 40 cells)	354.0 ± 23.4
0–100 μm	69.7 ± 9.1 (*n* = 23)	92.8 ± 13.9	9.8 ± 0.6 (*n* = 30)	190.1 ± 15.7
100–200 μm	58.9 ± 6.8 (*n* = 25)	88.4 ± 12.3	8.1 ± 0.5 (*n* = 34)	130.4 ± 14.1
200–300 μm	45.6 ± 5.6 (*n* = 30)	83.2 ± 11.7	8.1 ± 0.4 (*n* = 33)	115.2 ± 11.6
Doxycycline/GSK-3 inhibitor IX				
Marginal	12.6 ± 2.5 (*n* = 21 slides)	100	11.8 ± 2.2 (*n* = 12 cells)	193.1 ± 37.6
0–100 μm	32.1 ± 7.4 (*n* = 18)	57.1 ± 10.2	6.7 ± 0.5 (*n* = 19)	70.2 ± 11.5
100–200 μm	24.8 ± 4.2 (*n* = 17)	49.0 ± 8.5	5.9 ± 0.4 (*n* = 22)	58.0 ± 5.8
200–300 μm	27.7 ± 3.3 (*n* = 20)	39.3 ± 7.5	6.2 ± 0.5 (*n* = 21)	62.8 ± 7.5
Doxycycline/SB415286				
Marginal	21.3 ± 4.9 (*n* = 27 slides)	100	9.8 ± 0.5 (*n* = 20 cells)	260.6 ± 25.5
0–100 μm	44.7 ± 5.6 (*n* = 19)	67.7 ± 15.2	7.2 ± 0.6 (*n* = 21)	90.4 ± 15.6
100–200 μm	30.8 ± 3.9 (*n* = 24)	65.6 ± 10.3	6.1 ± 0.4 (*n* = 36)	71.2 ± 12.4
200–300 μm	20.5 ± 3.50 (*n* = 19)	63.4 ± 12.1	6.0 ± 0.5 (*n* = 15)	58.0 ± 6.4
ARF6-CA/DMSO				
Marginal	89.8 ± 13.5 (*n* = 20 slides)	100	11.6 ± 0.5 (*n* = 24 cells)	208.5 ± 17.8
0–100 μm	89.5 ± 13.2 (*n* =14)	73.2 ± 10.7	11.0 ± 1.2 (*n* = 17)	153.6 ± 19.0
100–200 μm	91.3 ± 16.0 (*n* =19)	47.3 ± 9.0	13.2 ± 1.5 (*n* = 18)	196.3 ± 30.0
200–300 μm	71.8 ± 19.8 (*n* =13)	60.7 ± 12.3	13.1 ± 3.0 (*n* = 15)	136.6 ± 23.7
ARF6-CA/GSK-3 inhibitor IX				
Marginal	56.1 ± 10.2 (*n* = 19 slides)	100	8.8 ± 1.0 (*n* = 10 cells)	131.2 ± 22.5
0–100 μm	63.6 ± 13.1 (*n* = 17)	51.4 ± 13.8	13.7 ± 1.9 (*n* = 18)	123.2 ± 13.9
100–200 μm	60.5 ± 7.6 (*n* = 20)	51.9 ± 10.2	13.4 ± 1.5 (*n* = 27)	138.9 ± 12.9
200–300 μm	66.7 ± 12.6 (*n* = 16)	45.5 ± 11.7	14.1 ± 1.9 (*n* = 21)	130.0 ± 13.5
ARF6-CA/SB415286				
Marginal	76.6 ± 9.0 (*n* = 24 slides)	100	10.6 ± 0.7 (*n* = 28 cells)	191.5 ± 19.1
0–100 μm	62.5 ± 10.31 (*n* = 17)	47.1 ± 10.7	12.3 ± 1.4 (*n* = 17)	143.3 ± 15.3
100–200 μm	56.8 ± 8.9 (*n* = 21)	58.7 ± 10.1	16.0 ± 1.9 (*n* = 25)	198.4 ± 26.7
200–300 μm	56.4 ± 9.7 (*n* = 14)	61.3 ± 13.9	16.9 ± 2.3 (*n* = 14)	224.9 ± 38.3

These data were derived from images like those shown in Fig. 2. Confluent MDCK cell monolayers (1:10 ratio of GFP-actin-expressing to non-GFP-actin-expressing cells) were infected with adenovirus encoding HA-tagged ARF6-CA under the control of a tetracycline-responsive promoter in the presence or absence of doxycycline. Therefore, cells not expressing ARF6-CA are labeled "doxycycline," which prevents transgene expression in the Tet-Off system, while ARF6-CA-expressing cells are labeled "ARF6-CA." Following infection, the cells were treated with 0.2% DMSO carrier solvent, 2.5 μM GSK-3 inhibitor IX or 40 μM SB415286. The cells were fixed, permeabilized and stained for F-actin and the HA epitope 12 h after wounding.

[a] Distance from the margin was measured along a straight line from and perpendicular to the wound margin to each GFP-actin-expressing cell.

[b] Percentage of GFP-actin-expressing cells with measurable membrane protrusions in any direction was determined using those cells in a cluster of GFP-actin-expressing cells for which protrusions could be discerned projecting under neighboring cells divided by the total number of GFP-actin-expressing cells in each random field of view. Values are weighted average ± SEM. Each data set was derived from at least three independent experiments for this and all subsequent parameters.

[c] Percent of submarginal protrusions oriented toward the wound margin (within ± 60° of the axis perpendicular to the margin) was determined from the set of protruding cells. Values are weighted average ± SEM.

[d] Protrusion length at the margin was measured from the farthest point of the lamellipodial tip to the cell body, using phase-contrast micrographs, which allow for clear visualization of the border between cell body and protrusion for marginal cells. Submarginal protrusion length was measured from the farthest point of a basal protrusion extending from a GFP-actin-expressing cell to the TRITC-phalloidin-stained F-actin associated with the adhesion belt of the cell under which the protrusion projects (approximately the point of apical cell–cell contact).

[e] Protrusion area was determined concurrently with the length measurements in the preceding column for the same cells (mean ± SEM).

sheet migration with ARF6-CA-expressing cells treated with 40 μM SB4125286. The rate of cell sheet migration in inhibitor-treated wounded monolayers increased from 0.17 ± 0.01 μm/min (mean ± SEM) to 0.29 ± 0.02 μm/min with expression of ARF6-CA, with the normal untreated rate being 0.59 ± 0.02 μm/min, as shown in Fig. 1.

Expression of ARF6-CA does not result in normal levels of directional polarization of submarginal cells

Interestingly, while ARF6-CA expression results in greater frequency of protrusion than in controls, as mentioned above, the degree of orientation of submarginal cells' protrusions toward

the wound area is, in contrast, lower than in controls (ARF6-CA/DMSO compared to doxycycline/DMSO in Table 1). Furthermore, expression of ARF6-CA does not restore the high normal level of directional polarization of submarginal protrusions toward the wound in GSK-3 inhibitor-treated cells (Table 1). Clearly, ARF6-CA causes a relatively randomly oriented pattern of protrusion in submarginal cells.

These data imply that GSK-3 may signal to ARF6, which in turn results in lamellipodial protrusion, but that GSK-3's role in cell polarity is ARF6-independent and therefore is a separate branch of the GSK-3 pathway. However, since proper directional polarization of submarginal cells decreases with inhibition of GSK-3 in wounded MDCK cell monolayers, the role of GSK-3 in cell polarity in this case appears different from that in astrocytes, where it is the Cdc42-dependent inactivating phosphorylation of GSK-3 that allows for cell polarization [15]. It is possible that part of the effect of the GSK-3 inhibitors on the rate of wound closure is due to an effect on cell polarity, perhaps in directional sensing and orientation of new submarginal protrusions toward the wound area or in the maintenance of persistent polarization in that direction. This could explain why ARF6-CA only partially restores the normal rate of overall cell sheet migration in GSK-3 inhibitor-treated cells, since wound-directed polarization of submarginal cells may be required for efficient progress of the cell sheet as a whole as it advances into the wound area. However, our previous results have shown that microinjection of a dominant-negative version of Cdc42, a critical regulator of cell polarity (for reviews, see Refs. [10–14]), into the first three rows of cells from the wound margin does not affect the rate of MDCK cells sheet migration, although it does decrease the regularity and "smoothness" of the wound edge over the course of closure [18] (as does inhibition of the Rho pathway by a different mechanism [18,19]).

Silencing of GSK-3α or GSK-3β expression slows cell sheet migration

By Western blot analysis and RT-PCR, we found that both GSK-3α and GSK-3β are expressed in MDCK cells at similar levels (data not shown). We sought to silence the expression of GSK-3α and GSK-3β separately by isoform-specific siRNAs. We designed four different siRNAs for each isoform for expression in MDCK cells from stably transfected shRNA expression constructs. We calculated by laser densitometry that ~90% knockdown of GSK-3α (~50 kDa by Western blot analysis) and ~44% knockdown of GSK-3β (~45 kDa) were achieved with the best of each isoform-specific siRNA. We did not detect knockdown of a larger ~59-kDa GSK-3β protein, GSK-3β transcript variant 4, with the GSK-3β siRNA, although the target sequence used is also present in this transcript variant. However, this variant is constitutively phosphorylated (inactivated) in MDCK cells, as discussed further below. Knockdown of either GSK-3α or GSK-3β resulted in slowed cell sheet migration, with the silencing of GSK-3β having the stronger effect (Fig. 3). Since we achieved only moderate knockdown of GSK-3β (despite trying multiple GSK-3β siRNA target sequences), our data probably greatly understate the importance of GSK-3β in the regulation of cell sheet migration. The results therefore suggest that GSK-3, particularly GSK-3β, plays a significant role in cell migration during MDCK wound closure.

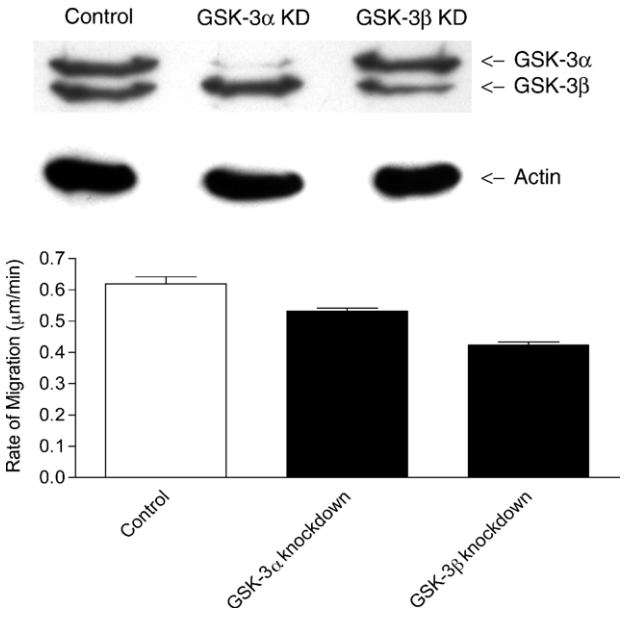

Fig. 3 – RNAi-based silencing of GSK-3α or GSK-3β expression slows cell sheet migration. The rate of overall cell sheet migration following wounding of confluent MDCK cell monolayers, as in Fig. 1, is expressed as mean ± SEM and derived from three separate experiments each for inert siRNA-expressing cells (control) and the GSK-3α siRNA-expressing cells, and four separate experiments for the GSK-3β siRNA-expressing cells. Efficiency of knockdown following stable transfection of the shRNA/siRNA expression constructs was evaluated by Western blot analysis of equivalent sample loadings with an anti-GSK-3α/β antibody, and an anti-actin antibody probe provided the loading control. These two siRNAs were the best of four siRNA target sequences for each isoform and yielded knockdowns of ~90% for GSK-3α (~50 kDa) and ~44% for GSK-3β (~45 kDa) by laser densitometry of Western blots. KD = knockdown.

Activity of GSK-3α and GSK-3β over the course of wound closure

GSK-3 is negatively regulated by phosphorylation on Ser 21 and Ser 9 of the α and β isoforms, respectively [1]. We analyzed the phosphorylation state of the GSK-3 isoforms as a function of time after wounding. The pattern of changes in phosphorylation state of GSK-3α over the course of wound closure appears more complex than that of GSK-3β. Both, however, are unphosphorylated (activated) over the most active phase of cell migration during wound closure.

In the unwounded MDCK cell monolayer, GSK-3α is in a completely unphosphorylated, activated state (Figs. 4A and B). Immediately upon wounding, GSK-3α becomes phosphorylated, detectable as early as 1-min post-wounding. This initial phosphorylation corresponds to a pre-migratory time frame, since the response to wounding normally involves a lag period before active cell migration and observable closure of the wound begins [19–21]. By 1 h, however, which corresponds to a time by which cells have started to extend lamellipodia and migrate, GSK-3α phosphorylation levels have dropped

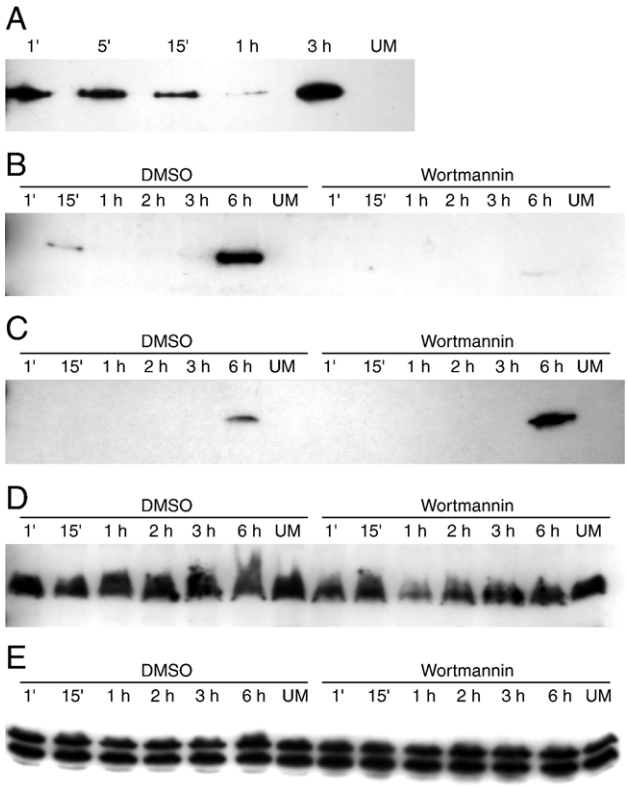

Fig. 4 – Both GSK-3α and GSK-3β are predominantly unphosphorylated (activated) during the most active migratory phase of the wound closure process. The data shown are Western blot analyses for phospho-GSK-3α, phospho-GSK-3β and total GSK-3α/β over the course of wound closure in confluent MDCK cell monolayers. (A) GSK-3α phosphorylation levels over the course of wound closure for narrow wounds that completely close by ~3 h. (B) GSK-3α phosphorylation levels over the course of wound closure for wider wounds that completely close by ~6 h. As indicated, the samples on the left half and the blots in panels C–E were treated with 0.02% DMSO carrier solvent alone prior to wounding, while those on the right half were treated with 200 nM wortmannin, a PI3K inhibitor. (C) ~45-kDa GSK-3β phosphorylation levels over the course of wound closure for wounds that completely close by ~6 h. (For narrower wounds that completely close by ~3, a single peak of GSK-3β phosphorylation is observed at 3 h.) (D) ~59-kDa GSK-3β transcript variant 4 phosphorylation levels over the course of wound closure for wounds that completely close by ~6 h. (E) Total GSK-3α (top band) and GSK-3β loading control for equivalent amounts of the same lysates as in panels B–D. Minutes after wounding are indicated with a tick mark. UM = unwounded monolayer.

dramatically (Figs. 4A and B). Finally, phosphorylation of GSK-3α increases again to very high levels by the time of complete wound closure (total coverage of the formerly open wound area): ~3 h for the narrow wounds made in the experiment shown in Fig. 4A. When we generated wider wounds that close ~6 h after wounding, we found that the second peak in GSK-3α phosphorylation occurs instead at 6 h (Fig. 4B), demonstrating that the second phase of GSK-3α phosphorylation depends upon closure of the wound and is not a fixed time-dependent phenomenon.

GSK-3β (~45 kDa) appears completely unphosphorylated (activated) throughout both the initial lag and the migratory phases of wound closure, as well as in the unwounded monolayer. However, GSK-3β does become phosphorylated by 3 h for narrower wounds (data not shown) and by 6 h for the wider wounds in Fig. 4C. For both sized wounds, this peak of phosphorylation again corresponds to the end of the wound closure process, when the former wound area is finally completely covered. In contrast, we found that a larger ~59-kDa GSK-3β protein, GSK-3β transcript variant 4 (RefSeq accession number XP_856691), was constitutively phosphorylated (inactivated) (Fig. 4D). The ~45-kDa GSK-3β protein could conceivably correspond to transcript variants 1, 2, 5, 6, 7 and/or 8, all of which are predicted to be between 43 and 48 kDa. Nevertheless, the regulation of the ~45-kDa GSK-3β and the ~59-kDa GSK-3β transcript variant 4 is clearly distinct.

Since GSK-3 can be regulated by phosphatidylinositol 3-kinase (PI3K)/Akt (also termed protein kinase B) pathway (for reviews, see Refs. [1–3]), we decided to test whether GSK-3 phosphorylation was sensitive to wortmannin, a selective PI3K inhibitor. The phosphorylation of GSK-3α, peaking soon after wounding and then again at the point of wound closure, was inhibited by treatment with 200 nM wortmannin (Fig. 4B). The ~45-kDa GSK-3β, on the other hand, actually appears higher with wortmannin treatment (Fig. 4D). Fig. 4E displays the total GSK-3α and GSK-3β proteins for each lysate—the same lysates for each treatment were used for all the experiments in Figs. 4B–D. We found that treatment of MDCK cell sheets with wortmannin or another PI3K inhibitor, LY294002, had no significant effect on wound closure at subtoxic concentrations (data not shown). This implies that the wortmannin-sensitive peaks in phosphorylation of GSK-3α reflect other processes that follow wounding, such as a stress response. It is also possible that the peak of inactivating phosphorylation of GSK-3α and/or GSK-3β at the end of the wound closure process may signal contact inhibition as the two opposing wound margins meet or the debut of the transient cell proliferation that occurs at a delay after wounding but does not contribute to wound closure [19].

Along with the GSK-3 inhibitor and RNAi data, these results are consistent with the notion that the unphosphorylated, activated forms of GSK-3α and/or GSK-3β (particularly the latter), which predominate during the migratory phase of wound closure, play a positive control or permissive function in MDCK cell sheet migration. This stands in contrast to the negative or non-permissive role GSK-3 plays in many other responses, where it is the inactivation of GSK-3 that allows the cell to respond to its stimulus (for reviews, see Refs. [1–3]).

Inhibition of GSK-3 strongly reduces Rac1 activation in HGF/SF-stimulated cells

Rac is a pivotal regulator of lamellipodial protrusion and membrane ruffling, among a host of other processes (for reviews, see Refs. [10–14]). We have previously shown that Rac function is critical for MDCK cell sheet migration, based on microinjection of dominant-negative Rac1 into the first three

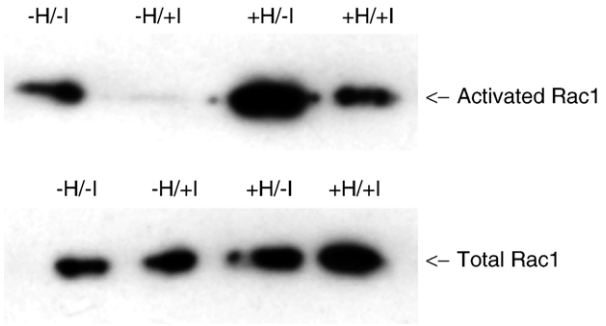

Fig. 5 – Inhibition of GSK-3 reduces basal and HGF/SF-stimulated levels of activated Rac1. Subconfluent MDCK cell cultures (~40% confluence, with cells in isolated multi-cell "islands") were treated with or without HGF/SF in the presence or absence of GSK-3 inhibitors for 24 h before cell lysis, isolation of activated Rac1 and Western blot analysis. Top panel, activated Rac1; bottom panel, corresponding total Rac1. –H = 0.5% PBS (without HGF/SF); +H = 25 ng/ml HGF/SF; –I = 0.1% DMSO; +I = with 2.5 μM GSK-3 inhibitor IX.

rows of cells around the wound margin [18] and adenoviral infection of dominant-negative Rac1 (data not shown), and Rac is a downstream effector of ARF6 [23]. We therefore sought to evaluate changes in the activation state of Rac1 over the course of MDCK wound closure and determine the effects of GSK-3 inhibitors on its activation. However, we detected no clear difference in activated Rac1 levels upon wounding of confluent MDCK cell monolayers above the basal level of unwounded monolayers (data not shown). In the present study, we made as many wounds as possible without causing damage to or lift-off of the entire monolayer, as described in Materials and methods. However, the majority of cells still do not abut a wound edge (the distance between wounds was ~3 mm, while the average cell diameter of MDCK cells is ~20 μm). For this reason, a wound-edge-localized difference in Rac1 activity may not be detectable in this experimental system. Alternatively, Rac1 activity may be permissive and necessary for wound closure without substantial changes in overall activity. It is known that Rac function is required constitutively for maintenance of adherens junctions in the continuous MDCK cell sheet [37,38]. Furthermore, there is protrusive activity even in the unwounded MDCK cell monolayer, with cells engaging in slow active "jostling" movements driven by actin polymerization and cryptic membrane protrusion [19], which implies a basal state of active cell motility even in a "quiescent" monolayer.

Rac function is also critical for MDCK cell scatter induced by HGF/SF [39], as is ARF6 [35]. We found that GSK-3 inhibitors inhibit cell scatter in cultures of subconfluent MDCK cells in response to HGF/SF, with the inhibitor-treated cells being less protrusive and less migratory than control cells (data not shown). HGF/SF induces an epithelial–mesenchymal-like transition in two-dimensional cultures of epithelial cells, with dissolution of cell–cell contacts and scatter of epithelial cells as highly migratory fibroblast-like individual cells [24–26]. We therefore assessed the levels of activated Rac1 in subconfluent MDCK cell cultures upon stimulation with HGF/SF in the presence and absence of GSK-3 inhibitors. In unstimulated cells, there is a low level of Rac1 activation, which is abrogated by treatment with 2.5 μM GSK-3 inhibitor IX (Fig. 5). Upon HGF/SF stimulation, there is a sharp increase in activated Rac1 levels, and this is again strongly reduced by treatment with 2.5 μM GSK-3 inhibitor IX (Fig. 5). Similar results were found with 40 μM SB415286 (data not shown).

Integration into a signaling hierarchy

A schematic diagram of the pathways leading to wound closure in MDCK cell sheets is shown in Fig. 6. The present study defines GSK-3, especially GSK-3β, as a positive control

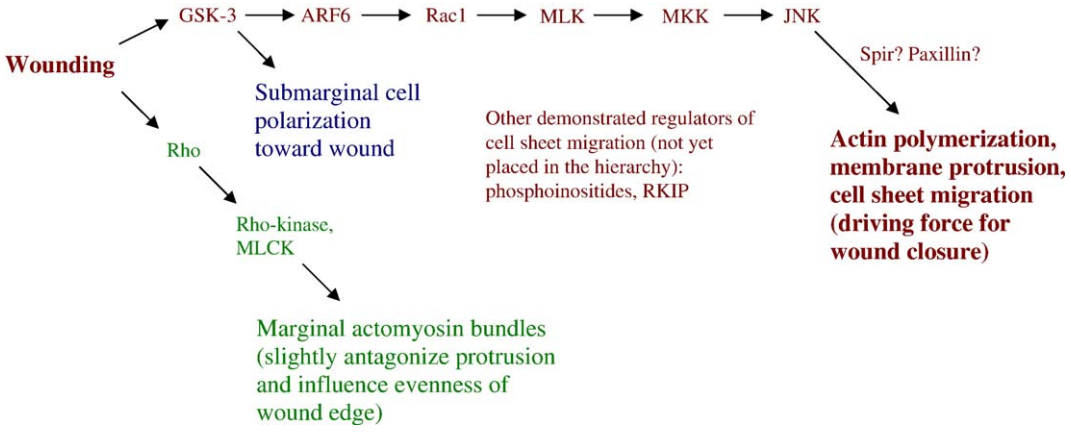

Fig. 6 – Schematic diagram of signal transduction pathways involved in wound closure in MDCK cell sheets. The pathway to cell migration, the main driving force for wound closure, is shown in red. Ancillary pathways that control the regularity of wound closure (green) and polarization of submarginal cells toward the wound area (blue) are also shown. This model for MDCK wound closure is supported by data from this study and Refs. [18–23,36]. Abbreviations not defined in the text: MLK, mixed-lineage kinase; MKK, MAP kinase kinase; JNK, c-Jun N-terminal kinase; RKIP, Raf kinase inhibitor protein. There are two mammalian homologs of *Drosophila* Spir (also known as Spire), which has been shown to have actin-nucleation activity and is regulated by JNK [40–43]. The activity of the cell adhesion protein paxillin is also regulated by JNK [44].

and perhaps permissive component of the signaling pathway to epithelial cell migration and suggests that it is integrated into the signaling hierarchy upstream of ARF6 and Rac1. In addition, a separate ARF6-independent branch of the GSK-3 pathway also acts positively to establish or maintain directional polarization of submarginal cells in the migrating cell sheet.

Acknowledgments

We thank James E. Casanova (University of Virginia) for adenoviral DNA and HA-tagged ARF6-CA (ARF6Q67L). We also thank Richard A. Cerione (Cornell University) for pGEX-KG-PBD (PAK3). This work was supported by a grant from the American Cancer Society (RZG-02-250-01-DDC) to G.F.

REFERENCES

[1] B.W. Doble, J.R. Woodgett, GSK-3: tricks of the trade for a multi-tasking kinase, J. Cell Sci. 116 (2003) 1175–1186.
[2] R.S. Jope, G.V. Johnson, The glamour and gloom of glycogen synthase kinase-3, Trends Biochem. Sci. 29 (2004) 95–102.
[3] S. Patel, B. Doble, J.R. Woodgett, Glycogen synthase kinase-3 in insulin and Wnt signalling: a double-edged sword? Biochem. Soc. Trans. 32 (2004) 803–808.
[4] J. Van Wauwe, B. Haefner, Glycogen synthase kinase-3 as drug target: from wallflower to center of attention, Drug News Perspect. 16 (2003) 557–565.
[5] J.R. Woodgett, Physiological roles of glycogen synthase kinase-3: potential as a therapeutic target for diabetes and other disorders, Curr. Drug. Targets Immune Endocr. Metabol. Disord. 3 (2003) 281–290.
[6] M. Alonso, A. Martinez, GSK-3 inhibitors: discoveries and developments, Curr. Med. Chem. 11 (2004) 755–763.
[7] P. Cohen, M. Goedert, GSK3 inhibitors: development and therapeutic potential, Nat. Rev., Drug Discov. 3 (2004) 479–487.
[8] L. Meijer, M. Flajolet, P. Greengard, Pharmacological inhibitors of glycogen synthase kinase 3, Trends Pharmacol. Sci. 25 (2004) 471–480.
[9] A. Harwood, V.M. Braga, Cdc42 and GSK-3: signals at the crossroads, Nat. Cell Biol. 5 (2003) 275–277.
[10] K. Burridge, K. Wennerberg, Rho and Rac take center stage, Cell 116 (2004) 167–179.
[11] M. Schwartz, Rho signalling at a glance, J. Cell Sci. 117 (2004) 5457–5458.
[12] K. Wennerberg, C.J. Der, Rho-family GTPases: it's not only Rac and Rho (and I like it), J. Cell Sci. 117 (2004) 1301–1312.
[13] A.B. Jaffe, A. Hall, Rho GTPases: biochemistry and biology, Annu. Rev. Cell Dev. Biol. 21 (2005) 247–269.
[14] E.M. Sorokina, J. Chernoff, Rho-GTPases: new members, new pathways, J. Cell. Biochem. 94 (2005) 225–231.
[15] S. Etienne-Manneville, A. Hall, Cdc42 regulates GSK-3β and adenomatous polyposis coli to control cell polarity, Nature 421 (2003) 753–756.
[16] L. Koivisto, K. Alavian, L. Hakkinen, S. Pelech, C.A. McCulloch, H. Larjava, Glycogen synthase kinase-3 regulates formation of long lamellipodia in human keratinocytes, J. Cell Sci. 116 (2003) 3749–3760.
[17] L. Koivisto, L. Hakkinen, K. Matsumoto, C.A. McCulloch, K.M. Yamada, H. Larjava, Glycogen synthase kinase-3 regulates cytoskeleton and translocation of Rac1 in long cellular extensions of human keratinocytes, Exp. Cell Res. 293 (2004) 68–80.
[18] G. Fenteany, P.A. Janmey, T.P. Stossel, Signaling pathways and cell mechanics involved in wound closure by epithelial cell sheets, Curr. Biol. 10 (2000) 831–838.
[19] R. Farooqui, G. Fenteany, Multiple rows of cells behind an epithelial wound edge extend cryptic lamellipodia to collectively drive cell-sheet movement, J. Cell Sci. 118 (2005) 51–63.
[20] Z.M. Altan, G. Fenteany, c-Jun N-terminal kinase regulates lamellipodial protrusion and cell sheet migration during epithelial wound closure by a gene expression-independent mechanism, Biochem. Biophys. Res. Commun. 322 (2004) 56–67.
[21] K.T. Mc Henry, S.V. Ankala, A.K. Ghosh, G. Fenteany, A non-antibacterial oxazolidinone derivative that inhibits epithelial cell sheet migration, ChemBioChem 11 (2002) 1105–1111.
[22] S. Zhu, K.T. Mc Henry, W.S. Lane, G. Fenteany, A chemical inhibitor reveals the role of Raf kinase inhibitor protein in cell migration, Chem. Biol. 12 (2005) 981–991.
[23] L.C. Santy, J.E. Casanova, Activation of ARF6 by ARNO stimulates epithelial cell migration through downstream activation of both Rac1 and phospholipase D, J. Cell Biol. 154 (2001) 599–610.
[24] M. Stoker, Effect of scatter factor on motility of epithelial cells and fibroblasts, J. Cell. Physiol. 139 (1989) 565–569.
[25] M. Stoker, E. Gherardi, M. Perryman, J. Gray, Scatter factor is a fibroblast-derived modulator of epithelial cell mobility, Nature 327 (1987) 239–242.
[26] M. Stoker, M. Perryman, An epithelial scatter factor released by embryo fibroblasts, J. Cell Sci. 77 (1985) 209–223.
[27] K.M. Weidner, J. Behrens, J. Vandekerckhove, W. Birchmeier, Scatter factor: molecular characteristics and effect on the invasiveness of epithelial cells, J. Cell Biol. 111 (1990) 2097–2108.
[28] C. Ballestrem, B. Wehrle-Haller, B.A. Imhof, Actin dynamics in living mammalian cells, J. Cell Sci. 111 (1998) 1649–1658.
[29] A.I. Barth, A.L. Pollack, Y. Altschuler, K.E. Mostov, W.J. Nelson, NH2-terminal deletion of ®-catenin results in stable colocalization of mutant β-catenin with adenomatous polyposis coli protein and altered MDCK cell adhesion, J. Cell Biol. 136 (1997) 693–706.
[30] Y. Altschuler, S.M. Barbas, L.J. Terlecky, K. Tang, S. Hardy, K.E. Mostov, S.L. Schmid, Redundant and distinct functions for dynamin-1 and dynamin-2 isoforms, J. Cell Biol. 143 (1998) 1871–1881.
[31] S. Gopalakrishnan, M.A. Hallett, S.J. Atkinson, J.A. Marrs, Differential regulation of junctional complex assembly in renal epithelial cell lines, Am. J. Physiol.: Cell Physiol. 285 (2003) C102–C111.
[32] J.A. Glaven, I. Whitehead, S. Bagrodia, R. Kay, R.A. Cerione, The Dbl-related protein, Lfc, localizes to microtubules and mediates the activation of Rac signaling pathways in cells, J. Biol. Chem. 274 (1999) 2279–2285.
[33] L. Meijer, A.L. Skaltsounis, P. Magiatis, P. Polychronopoulos, M. Knockaert, M. Leost, X.P. Ryan, C.A. Vonica, A. Brivanlou, R. Dajani, C. Crovace, C. Tarricone, A. Musacchio, S.M. Roe, L. Pearl, P. Greengard, GSK-3-selective inhibitors derived from Tyrian purple indirubins, Chem. Biol. 10 (2003) 1255–1266.
[34] M.P. Coghlan, A.A. Culbert, D.A. Cross, S.L. Corcoran, J.W. Yates, N.J. Pearce, O.L. Rausch, G.J. Murphy, P.S. Carter, L. Roxbee Cox, D. Mills, M.J. Brown, D. Haigh, R.W. Ward, D.G. Smith, K.J. Murray, A.D. Reith, J.C. Holder, Selective small molecule inhibitors of glycogen synthase kinase-3 modulate glycogen metabolism and gene transcription, Chem. Biol. 7 (2000) 793–803.
[35] F. Palacios, L. Price, J. Schweitzer, J.G. Collard, C. D'Souza-Schorey, An essential role for ARF6-regulated membrane traffic in adherens junction turnover and epithelial cell migration, EMBO J. 20 (2001) 4973–4986.

[36] L.C. Santy, K.S. Ravichandran, J.E. Casanova, The DOCK180/Elmo complex couples ARNO-mediated Arf6 activation to the downstream activation of Rac1, Curr. Biol. 15 (2005) 1749–1754.
[37] S. Kuroda, M. Fukata, K. Fujii, T. Nakamura, I. Izawa, K. Kaibuchi, Regulation of cell–cell adhesion of MDCK cells by Cdc42 and Rac1 small GTPases, Biochem. Biophys. Res. Commun. 240 (1997) 430–435.
[38] K. Takaishi, T. Sasaki, H. Kotani, H. Nishioka, Y. Takai, Regulation of cell–cell adhesion by rac and rho small G proteins in MDCK cells, J. Cell Biol. 139 (1997) 1047–1059.
[39] A.J. Ridley, P.M. Comoglio, A. Hall, Regulation of scatter factor/hepatocyte growth factor responses by Ras, Rac, and Rho in MDCK cells, Mol. Cell. Biol. 15 (1995) 1110–1122.
[40] E. Kerkhoff, J.C. Simpson, C.B. Leberfinger, I.M. Otto, T. Doerks, P. Bork, U.R. Rapp, T. Raabe, R. Pepperkok, The Spir actin organizers are involved in vesicle transport processes, Curr. Biol. 11 (2001) 1963–1968.
[41] I.M. Otto, T. Raabe, U.E. Rennefahrt, P. Bork, U.R. Rapp, E. Kerkhoff, The p150-Spir protein provides a link between c-Jun N-terminal kinase function and actin reorganization, Curr. Biol. 10 (2000) 345–348.
[42] A. Wellington, S. Emmons, B. James, J. Calley, M. Grover, P. Tolias, L. Manseau, Spire contains actin binding domains and is related to ascidian posterior end mark-5, Development 126 (1999) 5267–5274.
[43] M.E. Quinlan, J.E. Heuser, E. Kerkhoff, R.D. Mullins, *Drosophila* Spire is an actin nucleation factor, Nature 433 (2005) 382–388.
[44] C. Huang, Z. Rajfur, C. Borchers, M.D. Schaller, K. Jacobson, JNK phosphorylates paxillin and regulates cell migration, Nature 424 (2003) 219–223.